

Journal of Materials Chemistry A

Materials for energy and sustainability

Accepted Manuscript

This article can be cited before page numbers have been issued, to do this please use: X. Lv, H. Chen, W. Zhou, S. Li and Z. Shao, *J. Mater. Chem. A*, 2020, DOI: 10.1039/D0TA02435J.



This is an Accepted Manuscript, which has been through the Royal Society of Chemistry peer review process and has been accepted for publication.

Accepted Manuscripts are published online shortly after acceptance, before technical editing, formatting and proof reading. Using this free service, authors can make their results available to the community, in citable form, before we publish the edited article. We will replace this Accepted Manuscript with the edited and formatted Advance Article as soon as it is available.

You can find more information about Accepted Manuscripts in the [Information for Authors](#).

Please note that technical editing may introduce minor changes to the text and/or graphics, which may alter content. The journal's standard [Terms & Conditions](#) and the [Ethical guidelines](#) still apply. In no event shall the Royal Society of Chemistry be held responsible for any errors or omissions in this Accepted Manuscript or any consequences arising from the use of any information it contains.

ARTICLE

CO₂-tolerant SrCo_{0.8}Fe_{0.15}Zr_{0.05}O_{3-δ} cathode for proton-conducting solid oxide fuel cellsXiuqing Lv,^{a,b} Huili Chen,^{*a} Wei Zhou,^c Si-Dian Li^a and Zongping Shao^cReceived 00th January 20xx,
Accepted 00th January 20xx

DOI: 10.1039/x0xx00000x

SrCo_{0.8}Fe_{0.2}O_{3-δ} (SCF) exhibits high ionic-electronic conductivity. However, its instability in the presence of CO₂ restricts its application in electrochemical devices. In this study, 5 mol% zirconium was introduced into SCF to promote its structural stability and CO₂ tolerance. SrCo_{0.8}Fe_{0.15}Zr_{0.05}O_{3-δ} (SCFZ) showed metallic electrical conductivity above 500 °C. Further, X-ray diffractometer and CO₂-temperature programmed desorption experiments indicated that SCFZ possessed adequate structural stability and CO₂ tolerance. The oxygen reduction activity and CO₂ tolerance were studied using a symmetrical cell SCFZ|BaZr_{0.1}Ce_{0.7}Y_{0.1}Yb_{0.1}O_{3-δ}(BZCYyb)|SCFZ. The electrochemical performances of SCFZ material as a cathode were investigated systematically for proton-conducting solid oxide fuel cells (H⁺-SOFCs) with a configuration of NiO-BZCYyb|BZCYyb|SCFZ-BZCYyb. The output of 712 mW cm⁻² at 700 °C and a durability test of over 300 h indicated that SCFZ had significant structural stability and CO₂-tolerance.

Introduction

Solid oxide fuel cells (SOFCs) are promising power generation devices that directly convert chemical energy stored in fuels into electricity through an electrochemical reaction. The process is highly efficient and clean, with broad fuel adaptability.^{1,2} Nevertheless, operation of traditional SOFCs at high temperatures (850–1000 °C) leads to several issues, such as electrode sintering, interfacial reaction, high cost of components, and poor durability.³ Therefore, it has been a trend to lower the operating temperature of SOFC.^{4,5}

As a potential alternative, the proton-conducting SOFCs (H⁺-SOFCs) have been extensively investigated because of a lower activation energy of proton transportation than that of oxygen ion transportation; a low activation energy implies that the proton conductivity of these materials has less temperature dependence. Moreover, water is formed at the cathode rather than the anode, which avoids the dilution of the fuel and decreases the electrode polarization arising from mass transfer at the anode.⁶⁻⁸ BaZr_{0.1}Ce_{0.7}Y_{0.1}Yb_{0.1}O_{3-δ} (BZCYyb), which is highly proton-conductive and structurally stable in the intermediate-temperature (IT, 500–700 °C) range, has been regarded as an emerging electrolyte for IT-SOFCs.⁹⁻¹⁰ The cathode is another important consideration when the operating temperature needs to be reduced because the cathode polarization resistance increases at lower

temperatures. Therefore, developing structurally stable cathode materials with adequate electronic conductivity to reduce polarization resistance is crucial for IT-SOFCs.¹¹⁻¹³ The perovskite-type mixed ionic-electronic conductor (MIEC) materials are generally used as cathodes for SOFCs. Compared to a pure electronic conductor, such as lanthanum strontium manganate (LSM), a MIEC cathode effectively enlarges the area of oxygen reduction reaction (ORR) from the electrolyte/electrode interface to the entire cathode bulk.¹⁴⁻¹⁶ The cubic perovskite SrCoO_{3-δ} is a promising parent compound owing to its excellent catalytic activity for ORR, high ionic-electronic conductivity, and oxygen flux.^{15,17-18} However, for application as a cathode in SOFCs, SrCoO_{3-δ} is impeded by its low structural stability, especially in the presence of CO₂. These disadvantages can drastically decrease the cell performance.^{17,19,20} An effective way to increase its stability is to partially substitute the B-site ions with suitable dopants while maintaining its catalytic activity and desirable conductivity.²¹⁻²⁴ It has been reported that the partial substitution of Co with Fe, for instance, SrCo_{0.8}Fe_{0.2}O_{3-δ} (SCF), stabilizes the cubic perovskite phase and simultaneously exhibits high mixed ionic-electronic conductivity. However, the cubic SCF converts to the orthorhombic phase below 790 °C, which exhibits very low ionic conductivity.²⁴⁻²⁸ Another challenge associated with using SCF as a cathode is the sensitivity to CO₂.²⁹⁻³¹ There is a competition between O₂ and CO₂ for the active oxygen vacancies of the cathode surface. Therefore, carbonate formation could take place on the SCF surface over a long-time exposure to CO₂ atmosphere, further causing unrecoverable crystal structure damage.³²

Partial substitution of the B-site ions of perovskites with high valent transition metals can reduce the basicity and enhance CO₂ tolerance.^{22, 33-36} Zirconium dioxide (ZrO₂) has been used as a dopant to stabilize the structure of perovskites because of

^a Institute of Molecular Science, Key Laboratory of Materials for Energy Conversion and Storage of Shanxi Province, Shanxi University, Taiyuan 030006, P.R. China.
E-mail: huilichen@sxu.edu.cn.

^b College of Chemistry and Chemical Engineering, Jinzhong University, Jinzhong 030619, P.R. China.

^c State Key Laboratory of Materials-Oriented Chemical Engineering, College of Chemical Engineering, Nanjing Tech University, NO.30 Puzhu Road(S), Nanjing, 211816, P.R. China.

its stable oxidation state and low thermal conductivity. For example, Zr-doped $\text{SrCo}_{0.4}\text{Fe}_{0.6-x}\text{Zr}_x\text{O}_{3-6}$, $\text{SrCo}_{0.95-x}\text{Fe}_x\text{Zr}_{0.05}\text{O}_{3-6}$,³⁷ $\text{Ba}_{0.5}\text{Sr}_{0.5}(\text{Co}_{0.8-x}\text{Zr}_x)\text{Fe}_{0.2}\text{O}_{3-6}$,³⁸ and $\text{Ba}_{0.5}\text{Sr}_{0.5}\text{Co}_{0.8}\text{Fe}_{0.1}\text{Zr}_{0.1}\text{O}_{3-6}$ ³⁹ show high structural stability. Zr is also doped into SrFeO_{3-6} to enhance its stability, making it potentially suitable for use as a cathode.^{36, 40} Zr-doped perovskite-type materials have been used to fabricate cathodes of H^+ -SOFCs and such cathodes exhibit excellent electrochemical performance.⁴¹⁻⁴³ Zr has also been doped in SCF as $\text{SrCo}_{0.7}\text{Fe}_{0.2}\text{Zr}_{0.1}\text{O}_{3-6}$ to inhibit undesired phase deformation and improve CO_2 tolerance.³⁰ However, as the amount of Zr increases, conductivity and permeation flux decrease because the electron hopping conduction between X^{4+} to X^{3+} ($\text{X} = \text{Co}$ and Fe) becomes difficult owing to the stable Zr^{4+} .^{40, 44} As discussed above, it is expected that SCF doped with as little amount Zr as possible may promote the structural stability without significantly sacrificing the ionic conductivity of SCF.

In this study, a perovskite-type material $\text{SrCo}_{0.8}\text{Fe}_{0.15}\text{Zr}_{0.05}\text{O}_{3-6}$ (SCFZ) with 5 mol% Zr dopant in the B-site was synthesized. X-ray diffractometer (XRD) and CO_2 -temperature programmed desorption (CO_2 -TPD) experiments indicated that SCFZ possesses adequate structural stability and CO_2 tolerance. The electrochemical performance and CO_2 tolerance of SCFZ as a cathode for SOFCs with the BZCYYb electrolyte was systematically evaluated at IT operating conditions.

Experimental

Synthesis of powders

$\text{SrCo}_{0.8}\text{Fe}_{0.2}\text{O}_{3-6}$ (SCF), $\text{SrCo}_{0.8}\text{Fe}_{0.15}\text{Zr}_{0.05}\text{O}_{3-6}$ (SCFZ), and $\text{Ba}_{0.5}\text{Sr}_{0.5}\text{Co}_{0.8}\text{Fe}_{0.2}\text{O}_{3-6}$ (BSCF) powders were prepared via a modified Penichi method using citric acid (CA) and ethylenediaminetetraacetic acid (EDTA) as chelating reagents. Taking SCFZ as an example, the analytical grade nitrate salts of strontium, cobalt, iron, and zirconium were added into distilled water in a stoichiometric ratio according to the target product, followed by the addition of CA and EDTA in the total metal ions:CA:EDTA molar ratio of 1:1.5:1. Aqueous ammonia was used to adjust the pH value of the solution to ~ 7 . The solution was stirred and heated at 70°C to form a viscous sol. The sol was pre-treated at 300°C for 5 h and then calcined in air at 1000°C for 5 h. SCF was calcined at 1000°C for 10 h. BSCF were obtained after calcination for 5 h at 950°C .

The $\text{BaZr}_{0.1}\text{Ce}_{0.7}\text{Y}_{0.1}\text{Yb}_{0.1}\text{O}_{3-6}$ (BZCYYb) electrolyte powders were also synthesized using EDTA and CA. Analytical grade $\text{Ba}(\text{NO}_3)_2$, $\text{Zr}(\text{NO}_3)_4 \cdot 5\text{H}_2\text{O}$, $\text{Ce}(\text{NO}_3)_3 \cdot 6\text{H}_2\text{O}$, $\text{Y}(\text{NO}_3)_3 \cdot 6\text{H}_2\text{O}$, and $\text{Yb}(\text{NO}_3)_3 \cdot 6\text{H}_2\text{O}$ were first dissolved in distilled water. Then, EDTA and CA were added into the solution in a mole ratio of total metal ions:CA:EDTA of 1:2:1. The pH of the solution was adjusted to 6–7 using aqueous ammonia. The solution was heated at 70°C until a viscous gel formed, which was pre-treated at 300°C for 5 h and then calcined at 1100°C for 5 h under air to obtain the BZCYYb powders.

Cell fabrication

To prepare the SCFZ|BZCYYb|SCFZ symmetrical cell for impedance spectroscopy measurement, the BZCYYb pellet was

fabricated through dry pressing at a pressure of 200 MPa. First, 0.4 g of BZCYYb powders were pressed at 100 MPa for 1 min, followed by calcining in air for 5 h at 1400°C to densify the electrolyte pellet. The pellet was then surface-polished with sandpaper to a thickness of 0.7 mm. The SCFZ powders were added in a mixing solution of isopropanol, ethylene glycol, and glycerol, and subsequently ball-mixed to obtain the cathode slurry, which was then sprayed onto both sides of the BZCYYb pellet and calcined in air for 2 h at 1000°C . Finally, a diluted Ag paste was deposited on the cathode layer as the current collector.

The single cell NiO-BZCYYb|BZCYYb|SCFZ-BZCYYb was prepared via a co-pressing/sintering and cathode slurry spray deposition/sintering method. 0.4 g of anode powders consisting of NiO, BZCYYb, and pore former in a mass ratio of 6:4:1 were pressed at 100 MPa for 30 s to form an anode pellet. Next, 0.025 g of BZCYYb powders were homogeneously dispersed on the surface of the above pellet and pressed at 200 MPa to form the anode/electrolyte bilayer that was fired in air for 5 h at 1450°C . The cathode slurry comprising SCFZ and BZCYYb (in 7:3 mass ratio) with a certain amount of ethylene glycol, isopropanol, and glycerol was sprayed onto the electrolyte layer and sintered in air at 900°C for 2 h.

Characterization

The phase structures of the samples were determined using an X-ray diffractometer (Rigaku D/Max-RB) equipped with filtered $\text{CuK}\alpha$ radiation at room temperature. The XRD patterns were collected in a 2θ range of 20 – 80° with a step rate of 5°min^{-1} . To survey the chemical compatibility, a mixture of SCFZ and BZCYYb powders (1:1 wt ratio) was sintered in air for 10 h at 1000°C . The obtained powders were then identified using XRD. For comparison, the mixture of SCF and BZCYYb were also treated in the same manner and sintered at different temperatures.

The scanning electron microscopy (SEM) and energy dispersive X-ray (EDX) spectroscopy analyses of SCFZ powders and single cells were carried out using FESEM (JEOL, JSM-7001F).

To obtain the physical properties of samples, such as thermal expansion coefficients (TECs) and the electrical conductivities, the sample powders were pressed at 200 MPa into the dense rectangular bars with dimensions of 2 mm \times 5 mm \times 12 mm, followed by calcining for 5 h at 1200°C in air. Electrical conductivities were determined using the four-probe DC technique. The voltage and current were monitored on a digital source meter (Keithley 2420) with an interval of 25°C from 200 – 850°C in air. The TECs of the samples were determined on a dilatometer (Netzsch DIL 402C). From 100 to 1000°C with a 5°min^{-1} ramping rate in air using Al_2O_3 as a reference.

The CO_2 adsorption ability was evaluated by CO_2 -TPD. In these experiments, 0.05 g of the BSCF, SCF, or SCFZ sample was first pre-treated under CO_2 atmosphere for CO_2 adsorption at 500°C for 2 h. Subsequently, the sample was cooled and Ar was fed to remove the residual CO_2 . Next, the samples were

heated at a heating rate of $10\text{ }^{\circ}\text{C min}^{-1}$ under Ar atmosphere. The CO_2 intensity in the effluent gas was recorded using an online mass spectrometer (Hiden QIC-20).

The electrochemical performances were tested using an electrochemical workstation (Ivium Technologies B.V., Netherlands). To investigate the performance stability in CO_2 , the symmetrical cells were tested under air or 10 vol% CO_2 -containing air flowing at 100 mL min^{-1} (STP). The frequency range was $0.01\text{--}10^6\text{ Hz}$ with a 10 mV amplitude. The electrochemical performances of single cells were measured based on the four-probe method. Hydrogen was supplied to the anode with a flow rate of 80 mL min^{-1} for the performance tests. In the stability test, the flow rate of hydrogen was 15 mL min^{-1} . The flowing air was the oxidant. The electrochemical impedance spectra (EIS) of single cells was determined under an open circuit voltage (OCV) condition with the frequency range of $0.1\text{--}10^6\text{ Hz}$ and a voltage amplitude of 10 mV .

Results and discussion

Structural characterization of samples

The XRD patterns of the as-sintered Fe-doped SCF and Fe/Zr co-doped SCFZ are shown in Fig. 1(a). The profiles of SCFZ and SCF are particularly similar, showing a cubic perovskite structure. The locally magnified XRD patterns of SCF and SCFZ with the 2θ range from 30° to 35° are shown in Fig. 1(b). The peak of SCFZ was shifted to the lower 2θ direction compared with that of SCF, suggesting that the lattice had expanded because of the partial replacement of Zr^{4+} for $\text{Fe}^{3+}/\text{Fe}^{4+}$ cations owing to a larger radius of Zr^{4+} (0.72 \AA) than $\text{Fe}^{3+}/\text{Fe}^{4+}$ ($0.645\text{ \AA}/0.585\text{ \AA}$).⁴⁵ The ZrO_2 phase did not appear in the diffraction pattern, indicating that Zr was successfully doped into the oxide lattice. A cubic perovskite phase can be stabilized by doping Fe or Fe/Zr (0.05) into the B-sites of the $\text{SrCoO}_{3-\delta}$ system.

The cubic (space group Pm-3m) structures of SCFZ and SCF were further confirmed by their refinement profiles (Fig. 1(c) and (d)). The lattice parameter of SCFZ ($a = 3.88190\text{ \AA}$) was bigger than that of SCF ($a = 3.8599\text{ \AA}$), suggesting a lattice expansion owing to the doping of Zr into the SCF perovskite lattice. The low converged reliability factors of SCFZ ($R_p = 3.437\%$, $R_{wp} = 4.349\%$) and SCF ($R_p = 3.395\%$, $R_{wp} = 4.273\%$) indicated a good fitting between the experimental and calculated patterns. The Rietveld refinement results of XRD patterns of SCFZ and SCF are given in Table 1.

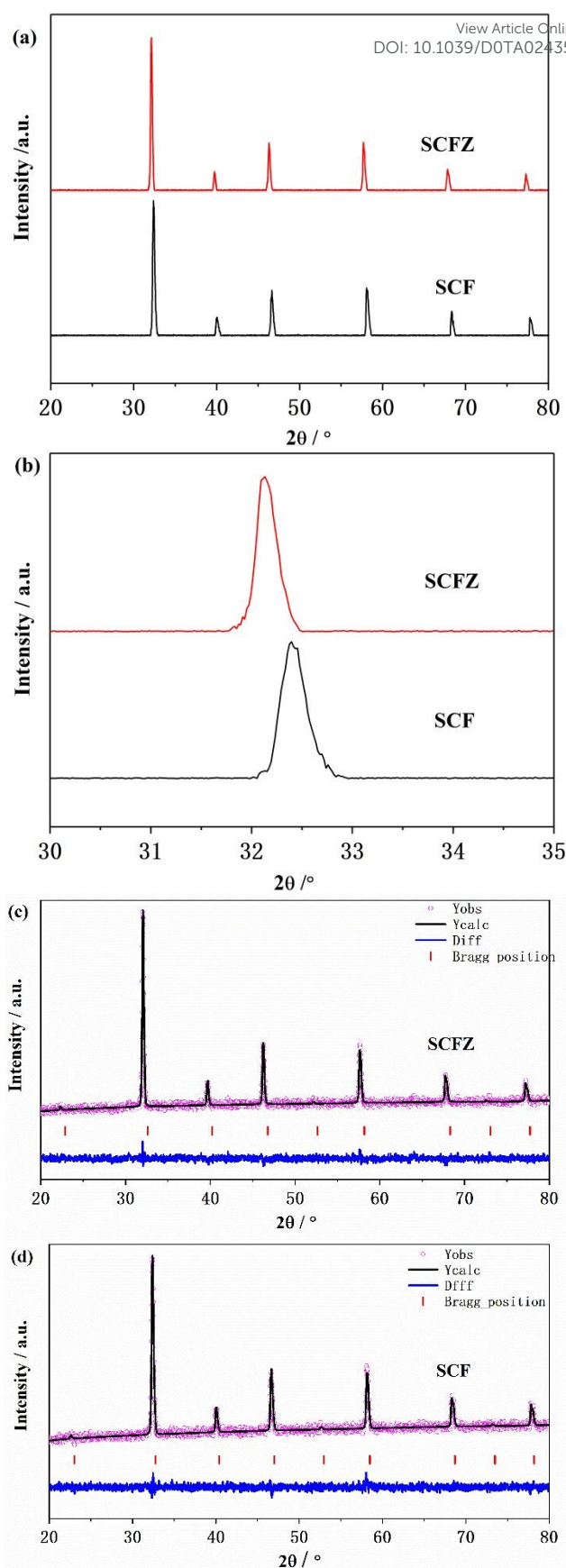


Fig. 1. (a) XRD patterns of as-sintered SCFZ and SCF. (b) Magnified XRD patterns of SCFZ and SCF in the 2θ range from 30° to 35° . Refined XRD profiles of (c) SCFZ and (d) SCF.

Table 1. Rietveld refinement results of XRD patterns of SCFZ and SCF.

Parameters	SCFZ	SCF
Space Group	Pm-3m	Pm-3m
a (Å)	3.88190(83)	3.8599(16)
b (Å)	3.88190(83)	3.8599(16)
c (Å)	3.88190(83)	3.8599(16)
α (°)	90	90
β (°)	90	90
γ (°)	90	90
Volume (Å ³)	58.495(38)	57.506(70)
R _{wp}	4.349%	4.273%
R _p	3.437%	3.395%
R _{exp}	4.147%	4.012%
G _{of}	1.049	1.065

Fig. 2 presents the morphology and EDS analysis of the SCFZ powders. As shown in Fig. 2(a), the sample includes five elements, i.e., Sr, Co, Fe, Zr, and O in the Sr:Co:Fe:Zr molar ratio of 1.01:0.82:0.15:0.05, which is close to the actual

stoichiometric ratio of 1:0.8:0.15:0.05. These results indicate that the stoichiometric target of SCFZ was successfully obtained.

The chemical compatibility between SCFZ and BZCYYb should be considered because the formation of new phases or even a non-conductive material at the interface would increase the ohmic resistance, and hence decrease the electrochemical performances of the cells. In addition, a weak adherence between the electrolyte and cathode layers may cause a large contact resistance and even delamination of the two layers. Fig. 3 shows that there was no new phase or peak shifts for the calcined SCFZ-BZCYYb mixture powders, which indicates that SCFZ had good chemical compatibility with BZCYYb during the operating temperature. For comparison, the phase-reaction between SCF and BZCYYb was also investigated. The impurity SrZrO_{3-δ} was detected in the product, indicating that SCF cannot be used as a cathode in SOFCs with the BZCYYb electrolyte. However, SCFZ can be considered in the fabrication of SOFCs based on the BZCYYb electrolyte.

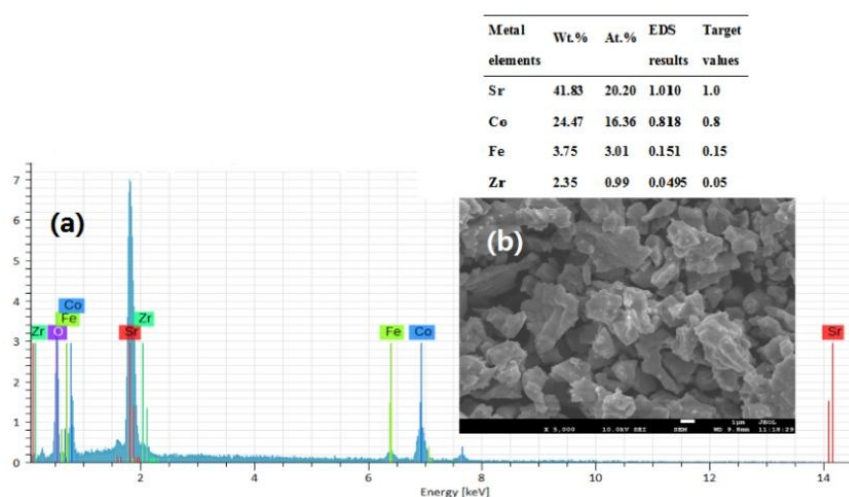


Fig. 2. (a) EDS analysis and (b) SEM image of SCFZ powders.

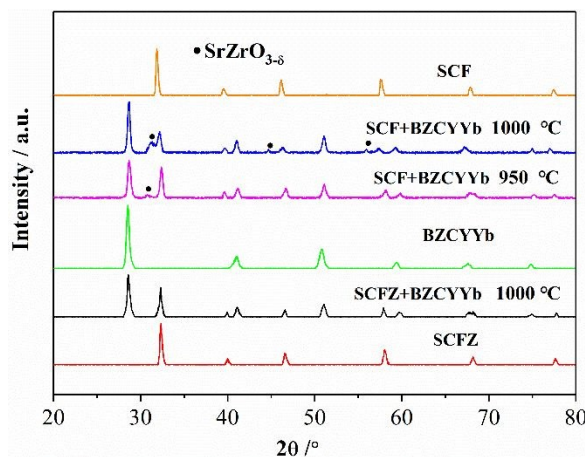


Fig. 3. XRD patterns of BZCYYb, SCFZ, and SCF; calcined SCFZ-BZCYYb (1:1 mass ratio) and SCF-BZCYYb (1:1 mass ratio).

Table 2. Conductivity, TEC, and E_a of reported cathode materials in literature and those of SCFZ prepared in this study

Cathode	Conductivity (maximum) (S cm ⁻¹)	E_a (kJ mol ⁻¹)	TEC × 10 ⁻⁶ (K ⁻¹)	Reference
BaCo _{0.4} Fe _{0.4} Zr _{0.2} O _{3-δ}	----	35.7 (300–450 °C) 23.1 (450–800 °C)	14.4 (100–1000 °C)	50
La _{0.6} Sr _{0.4} Co _{0.2} Fe _{0.8} O _{3-δ}	350	9.6 (100–500 °C)	15.3 (100–600 °C)	51
Ba _{0.5} Sr _{0.5} Co _{0.8} Fe _{0.2} O _{3-δ}	31	27.42 (30–800 °C)	20.44 (30–800 °C)	52
SrCo _{0.8} Fe _{0.15} Zr _{0.05} O _{3-δ}	345	7.4 (200–500 °C) 11.8 (500–850 °C)	26.01 (100–1000 °C)	This work

Table 3. Relative and real ASR change with time in air-10 vol% CO₂ atmosphere for reported cathode materials in literature and SCFZ materials prepared in this study.

Cathode	Electrolyte	ASR _t /ASR ₀ (times)		Slope (Ω cm ² min ⁻¹)	Reference
		5 min	1 h		
SrCo _{0.8} Nb _{0.1} Ta _{0.1} O _{3-δ}	Ce _{0.9} Gd _{0.1} O _{2-δ}	17	24	0.013	53
Ba _{0.5} Sr _{0.5} Co _{0.8} Fe _{0.2} O _{3-δ}	Ce _{0.9} Gd _{0.1} O _{2-δ}	30	45	0.045	53
SrCo _{0.85} Ta _{0.15} O _{3-δ}	Ce _{0.8} Sm _{0.2} O _{2-δ}	18	22	0.012	55
Ba _{0.5} Sr _{0.5} Co _{0.8} Fe _{0.2} O _{3-δ}	BaZr _{0.1} Ce _{0.7} Y _{0.1} Yb _{0.1} O _{3-δ}	30	44	0.045	This work
SrCo _{0.8} Fe _{0.15} Zr _{0.05} O _{3-δ}	BaZr _{0.1} Ce _{0.7} Y _{0.1} Yb _{0.1} O _{3-δ}	15	20	0.013	This work

Physical properties

The electrical conductivity of SrCoO_{3-δ}, SCF, and SCFZ in air is temperature-dependent (Fig. 4). SrCoO_{3-δ} has a hexagonal crystal structure and exhibits semiconductor-like character with 34 S cm⁻¹ conductivity at 850 °C. In contrast, SCF and SCFZ have a cubic perovskite structure and their electrical conductivities increase to a maximum with temperature and then decrease, which indicates a change from semiconductor-like character to metallic character. It is likely that this phenomenon is associated with the reduction of Co⁴⁺/Fe⁴⁺ to Co³⁺/Fe³⁺ that leads to the formation of oxygen vacancies.⁴⁶ SCFZ exhibits lower conductivity than SCF because the blocking effect of Zr⁴⁺ makes electron hopping conduction difficult after SCF is doped with Zr. Similar results have been reported for SrCo_{0.7}Fe_{0.2}Ta_{0.1}O_{3-δ}³⁴ and SrCo_{0.8}Fe_{0.1}Nb_{0.1}O_{3-δ},³⁵ in which Ta- or Nb-doping decreases the electrical conductivities of SCF. Although Zr-doping decreases the electrical conductivity of SCFZ, it is still significantly higher than that of an ideal SOFCs cathode (≥100 S cm⁻¹) in the IT range.⁴⁷ The Arrhenius plots of ln(σT) vs. 1000/T in the inset display a turning point (transition temperature), which demonstrates a small-polaron hopping conductor for SCFZ and SCF. In the case of SCFZ, the transition temperature (500 °C) is shifted toward higher temperature as compared to SCF (400 °C), indicating that oxygen loss becomes more difficult after Zr-doping into SCF, and the phase stability is further enhanced.⁴⁶ The activation energy (E_a) of the SCFZ sample in the high and low temperature ranges was 11.8 and 7.40 kJ mol⁻¹, respectively, calculated using the slope of the ln(σT) vs. 1000/T curve.

SrCoO_{3-δ}-based perovskites usually display large TECs, which might cause a mismatch between the electrolyte and cathode during heating and cooling. As shown in Fig. 5(a), the TECs for SCFZ and BZCYb were calculated to be 26.01 × 10⁻⁶ K⁻¹ and 10.18 × 10⁻⁶ K⁻¹, respectively. The TEC of SCFZ-BZCYb (7:3 mass ratio) was 20.63 × 10⁻⁶ K⁻¹, which lies between those of

SCFZ and BZCYb. Therefore, the incorporation of BZCYb into SCFZ enhances its thermal compatibility.

Fig. 5(b) shows the thermal expansion curves of SCF, BZCYb, and SCF-BZCYb (7:3 mass ratio). For the SCF cathode, the TEC was calculated to be 23.93 × 10⁻⁶ K⁻¹, which is lower than that of SCFZ (26.01 × 10⁻⁶ K⁻¹). As the ionic radius of Zr⁴⁺ is larger than those of Fe³⁺ and Fe⁴⁺, SCFZ had a larger unit-cell volume (58.495(38) Å³) than that of SCF (57.506(70) Å³). A larger volume is commonly associated with higher TECs.^{34, 48} The TEC of SCF-BZCYb (7:3 mass ratio) was 18.98 × 10⁻⁶ K⁻¹, which is the same value as that of SCFZ and between those of SCF and BZCYb.

It has been reported that there is an abrupt shape change in the curve of ΔL/L₀ vs. temperature (°C) for the SrCoO_{3-δ} oxide. The abrupt change takes place at 920 °C, which corresponds to structural phase transition at the elevated temperature.⁴⁹ However, there is no significant change in the curve of ΔL/L₀ vs. temperature(°C) for SCFZ, implying that the structural phase transition is prevented by introducing Fe and Zr.

The comparison of conductivity, TEC, and E_a of SCFZ with those of previously reported cathodes is given in Table 2.

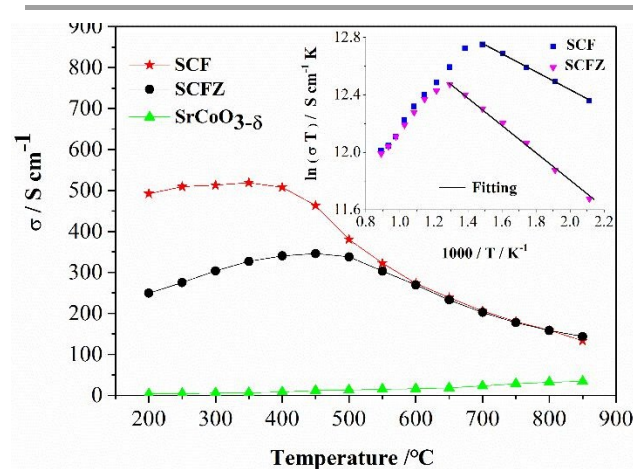


Fig. 4. Electrical conductivities of SrCoO_{3-δ}, SCFZ, and SCF in air. The inset displays the Arrhenius plot of $\ln(\sigma T)$ vs. $1000/T$.

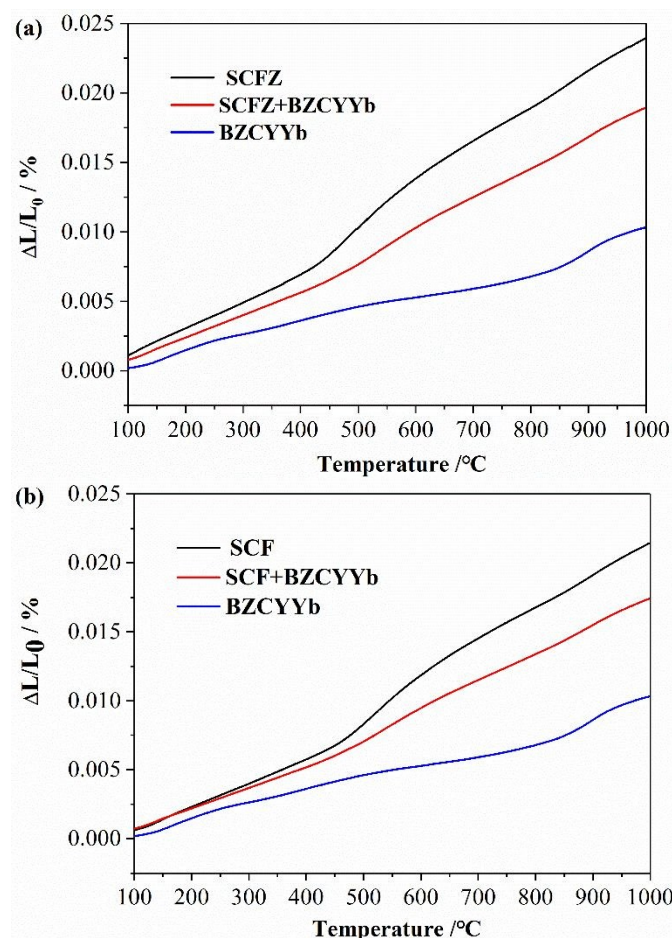


Fig. 5. Thermal expansion curves of (a) SCFZ, BZCYYb, and SCFZ-BZCYYb (7:3 mass ratio). (b) SCF, BZCYYb, and SCF-BZCYYb (7:3 mass ratio).

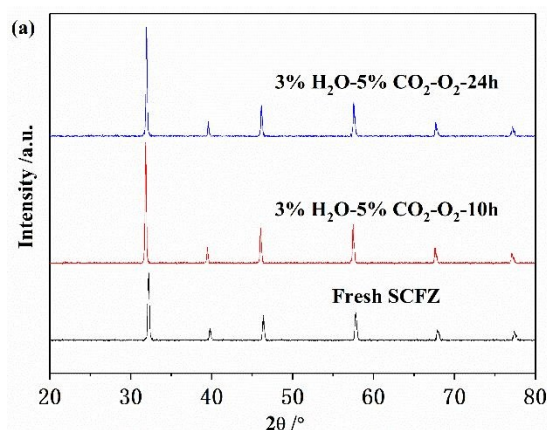
Structural stability under CO₂ exposure

When the cathode is in air, it is exposed to a small quantity of CO₂. Furthermore, in H⁺-SOFCs, water is formed at the cathode compartment. Thus, the cathode material must be structurally stable under CO₂ and H₂O conditions. The structural stability of SCFZ powders exposed to CO₂ and H₂O was investigated by treating the samples in 3% H₂O-5% CO₂-O₂ atmosphere at 700 °C for different time ranges. The XRD patterns of the fresh and treated samples are shown in Fig. 6(a) and 6(b), respectively. For comparison, the XRD patterns of SCF under the same conditions are displayed, where the additional peaks ascribed to SrCO₃ can be observed. As no carbonate phase was detected in the XRD spectra of SCFZ over 24 h, it was concluded that SCFZ had higher CO₂ tolerance relative to SCF.

The CO₂ adsorption ability of SCF and SCFZ was investigated by CO₂-TPD. As a comparison, BSCF was also surveyed in this test, which is a commonly used cathode for IT-SOFCs. As shown in Fig. 6(c), the BSCF sample gave a broad and strong peak from around 600 °C to 800 °C, which corresponded to the desorption of adsorbed CO₂ and decomposition of BaCO₃. The

areas of CO₂ desorption peaks for the SCF sample were much smaller than that of BSCF. According to the Lewis acid-base theory, Ba²⁺ has stronger basicity than Sr²⁺. Therefore, the partial substitution of Sr²⁺ with Ba²⁺ in BSCF will lead to higher basicity as compared to the complete Sr²⁺ occupation in the A-site of SCF. In addition, the formation of SrCO₃ is more difficult than the formation of BaCO₃ from barium/strontium perovskite oxide under a certain temperature and CO₂ pressure.^{53, 54} Unlike BSCF and SCF, SCFZ shows a significantly smaller CO₂ desorption peak at ~600 °C, which indicates a weaker CO₂ adsorption on the oxide surface.

Partial substitution of low valence Fe³⁺ by high valence Zr⁴⁺ enhanced the stability of SCF and suppressed the loss of oxygen from the lattice. Consequently, SCFZ exhibited a higher tolerance to CO₂ than SCF. Additionally, SCFZ had lower basicity than SCF. When zirconium was present at the B-sites of SCF, the substituted site showed more positive charge accompanied by a decrease in the number of oxygen vacancies, which increased the stability of oxygen atoms in the lattice, and decreased the basicity of the oxide. Therefore, the adsorption of acidic CO₂ on the oxide surface was lowered. These results revealed that SCFZ had the highest tolerance to CO₂ among the prepared cathode materials.



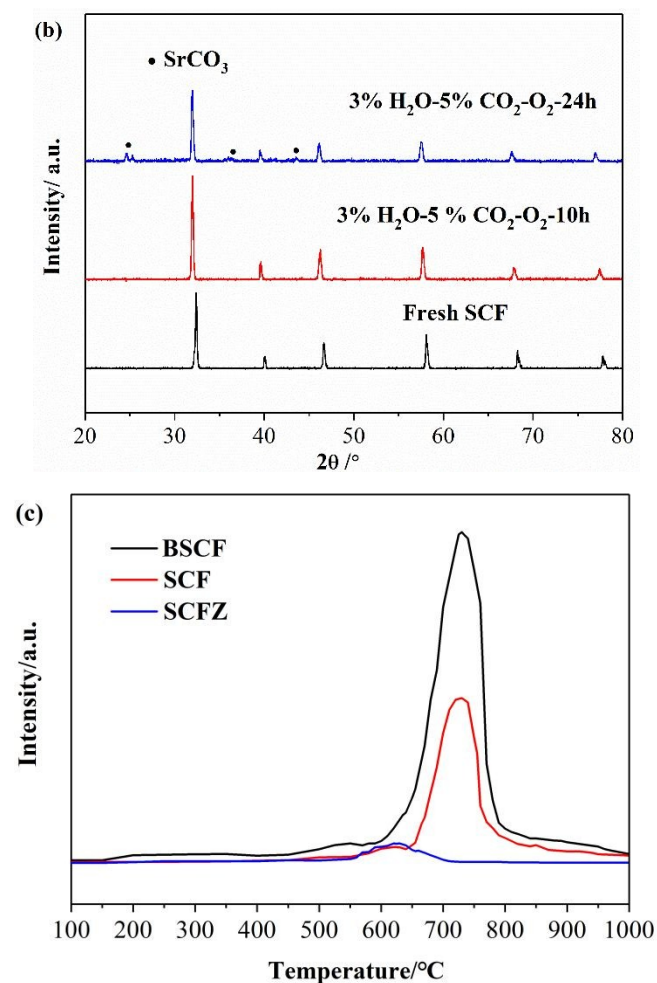


Fig. 6. XRD patterns of the fresh and treated samples of (a) SCFZ and (b) SCF in 3% H₂O-5% CO₂-O₂ at 700 °C. (c) CO₂-TPD profiles of SCFZ, SCF, and BSCF powders pre-treated in CO₂ at 500 °C for 2 h.

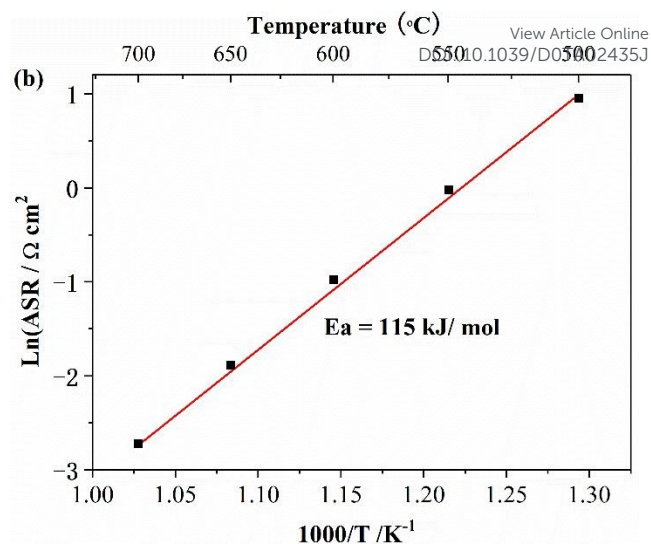
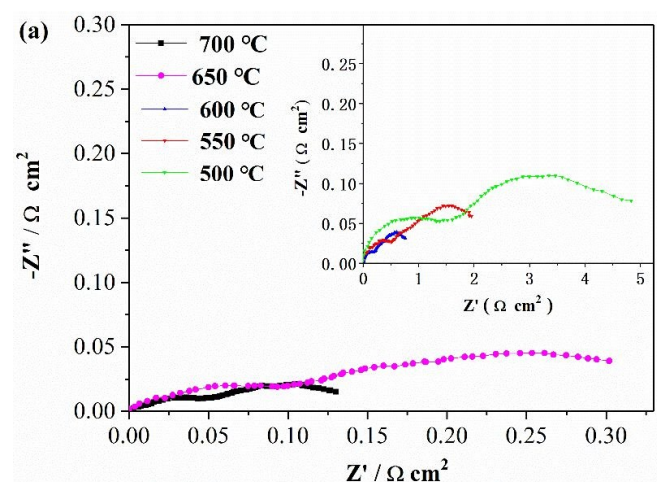


Fig. 7. (a) EIS of the symmetrical cell with SCFZ cathode on BZCYYb. (b) Arrhenius plot of the ASRs from 700 to 500 °C in air.

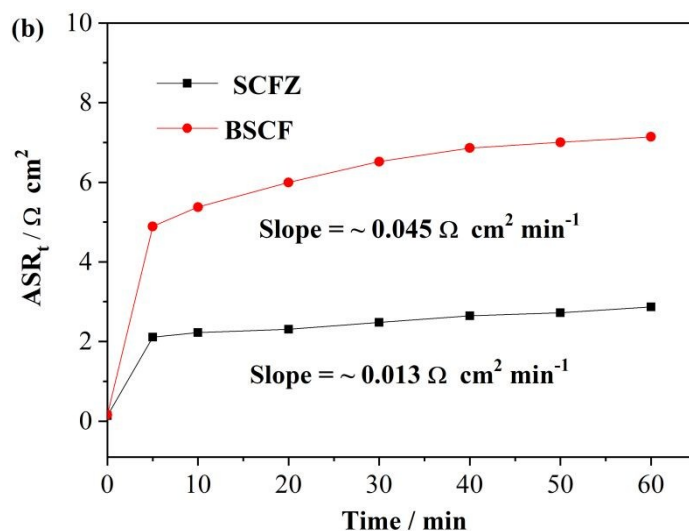
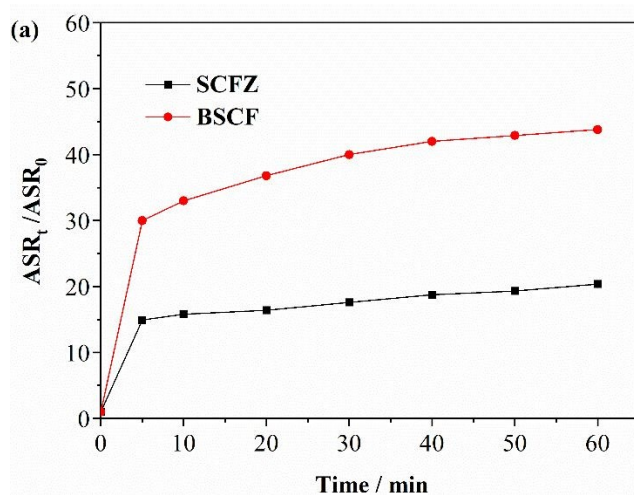


Fig. 8. (a) Relative and (b) real ASRs change with time for SCFZ and BSCF in air-10 vol% CO₂ atmosphere at 700 °C.

CO₂ tolerance of SCFZ in a symmetrical cell

The ORR activity of SCFZ as a cathode was tested using a symmetrical cell. Fig. 7(a) is the EIS of SCFZ|BZCYyb|SCFZ measured in air between 500 and 700 °C. The area specific resistances (ASRs) were obtained from the polarization resistance (R_p) of symmetrical cell, i.e., 2.42, 1.01, 0.38, 0.15, and 0.07 $\Omega \text{ cm}^2$ at 500, 550, 600, 650, and 700 °C, respectively. The ASR value is lower than that of $\text{BaCo}_{0.4}\text{Fe}_{0.4}\text{Zr}_{0.2}\text{O}_{3-\delta}$ (BCFZ) under the same conditions.⁴¹ As shown in Fig. 7(b), the activation energy of SCFZ was 113.7 kJ mol^{-1} , calculated using the slope of the $\ln(\text{ASR})$ vs. $1000/T$ curve, which was lower than that of the $\text{La}_{0.6}\text{Sr}_{0.4}\text{Co}_{0.2}\text{Fe}_{0.8}\text{O}_{3-\delta}$ (LSCF) based on the BZCYyb electrolyte (138 kJ mol^{-1}).⁴¹ This result indicates that SCFZ could be applied as a cathode material based on the electrolyte BZCYyb.

The degradation of cathode performance was evaluated at 700 °C as a function of time using a symmetrical cell SCFZ|BZCYyb|SCFZ in a gas mixture of air-10 vol% CO_2 . For comparison, the BSCF profile was also monitored under the same condition. The relative ASRs change (the recorded ASR_t against the initial ASR_0) are presented in Fig. 8(a). The relative ASRs change of BSCF increased by almost 30 times in the first 5 min and by 44 times after 1 h. The cathode performance of SCFZ was better than that of the BSCF cathode. After exposure for 5 min, ASR_t increased merely 15 times relative to ASR_0 . Beyond 1 h exposure, the degradation was slow and showed some linear tendency. Relative to ASR_0 , ASR_t increased by 20 times. Fig. 8(b) shows the real ASR change with time for SCFZ and BSCF; the increasing rate of ASRs for BSCF after 5 min was $\sim 0.045 \text{ } \Omega \text{ cm}^2 \text{ min}^{-1}$. However, the linear increasing rate of the ASRs for SCFZ after 5 min was $\sim 0.013 \text{ } \Omega \text{ cm}^2 \text{ min}^{-1}$, i.e., considerably lower than that of BSCF. The results suggested that SCFZ showed a significantly slower performance degradation compared to BSCF, which is used as a baseline cathode for IT-SOFCs. A comparison between the results of this work with those of previously reported CO_2 tolerant cathodes is given in Table 3.

Electrochemical performance

Fig. 9 shows the electrochemical performance (I-V-P) of the NiO-BZCYyb|BZCYyb|SCFZ-BZCYyb single cell from 700 to 500 °C. The OCV of 1.02 V at 700 °C indicated a densified electrolyte layer. The cell displayed peak power densities of 234, 353, 458, 551, and 712 mW cm^{-2} at 500, 550, 600, 650, and 700 °C, respectively, which were much higher than those of previously reported cells using LSCF and BCFZ cathodes with the electrolyte BZCYyb.⁴¹

For comparison, the I-V-P curves of the NiO-BCZYYb|BCZYYb|SCF-BZCYyb single cell were measured from 700 to 500 °C. As shown in Fig. 9(b), the peak power densities of the cell were 194, 294, 431, 549, and 719 mW cm^{-2} at 500, 550, 600, 650, and 700 °C, respectively. The peak power density at 700 °C was slightly higher than that of the SCFZ-based cell at this temperature. This result indicated that the cathode activity decreased only slightly as a result of Zr-doping. However, at other temperatures and with increasing time, the peak power densities of the SCFZ-based cell were higher than those of the SCF-based cell. This observation confirmed that Zr-doping greatly improved the CO_2 tolerance and stability of SCF.

Fig. 10a shows the EIS of the single cell from 500 to 700 °C. The high frequency intercept at the real axis corresponds to the ohmic resistance (R_o) of the electrolyte, electrodes, and lead wires. The total resistance (R_t) is the low frequency intercept at the real axis, and the difference of the intercepts of the high and low frequencies corresponds to the polarization resistance (R_p). All R_o , R_t , and R_p values of the cell decreased with the increasing temperature. The R_o and R_p values of the cell were 0.21, 0.29, 0.51, 0.62, and 0.80 $\Omega \text{ cm}^2$, and 0.05, 0.13, 0.29, 0.50, and 1.20 $\Omega \text{ cm}^2$ at 700, 650, 600, 550, and 500 °C, respectively. The proton conductivity of the electrolyte increased with increasing temperature, leading to a reduction in R_o . The Bode plot (Fig. 10b) shows that R_p decreased in the entire frequency region with the increasing temperature, especially in the low frequency region. This indicated faster electrode reaction dynamics and lower diffusion resistance at higher temperatures.

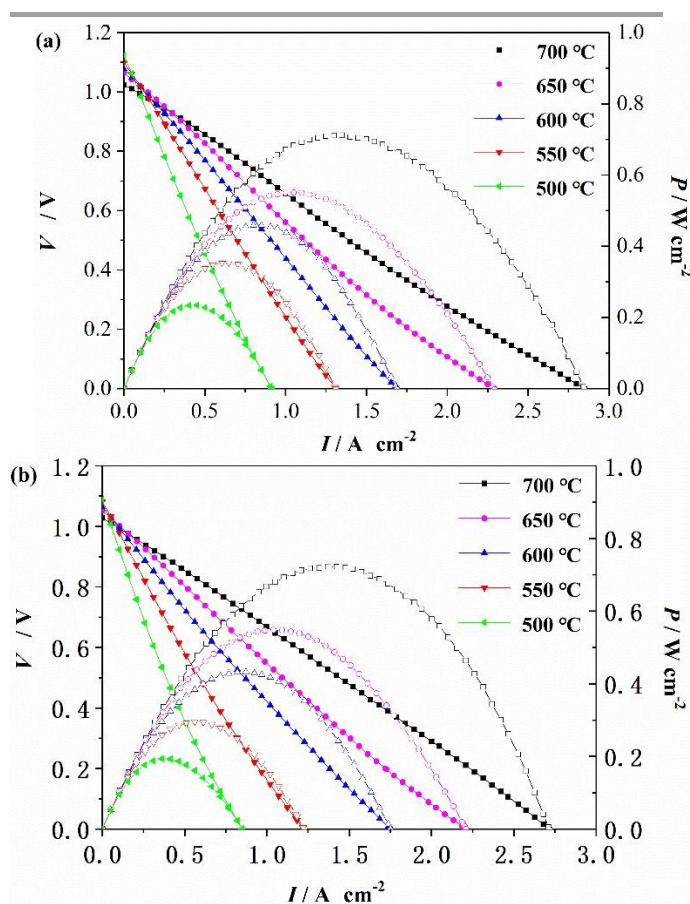


Fig. 9. I-V (P) curves of (a) NiO-BZCYyb|BZCYyb|SCFZ-BZCYyb and (b) NiO-BCZYYb|BCZYYb|SCF-BZCYyb cell from 700 to 500 °C.

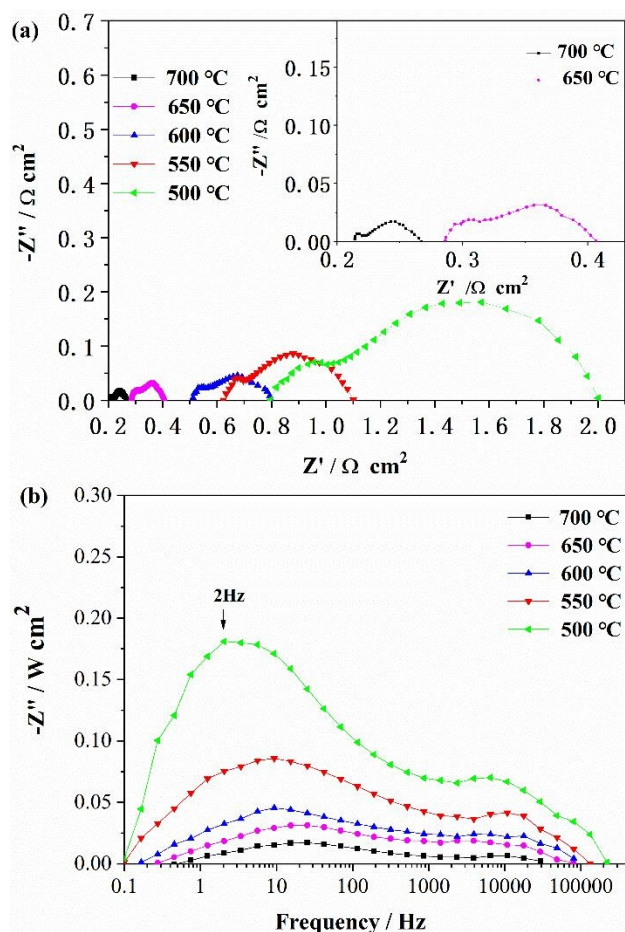


Fig. 10. (a) Nyquist and (b) Bode plot of EIS of the NiO-BZCYyb|BZCYyb|SCFZ-BZCYyb cell from 700 to 500 °C under flowing air as oxidant.

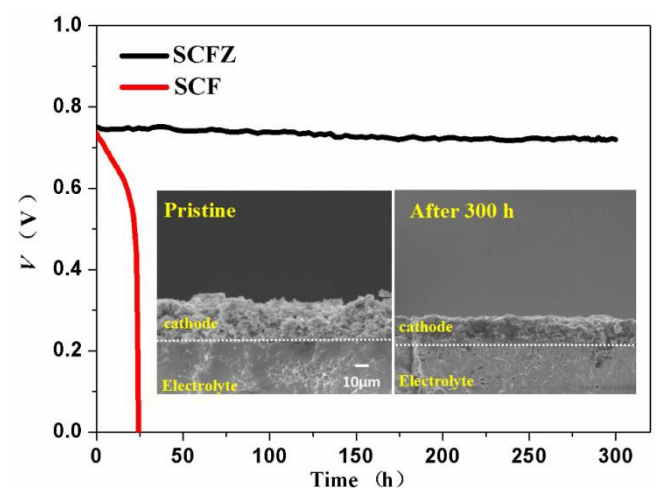


Fig. 11. Time-dependent voltage under a constant current density of 350 mA cm^{-2} at 600 °C of SCFZ- and SCF-based cells. The insets show the microstructure of the pristine and post-test SCFZ-based cells.

Aging test in the galvanostatic mode of the cell

To evaluate the stability of SCFZ as a cathode under real operating conditions, the cell voltage of the cell was monitored over time at 600 °C . For comparison, the SCF-based cell was

also tested. As shown in Fig. 11, under a constant current density of 350 mA cm^{-2} , the SCFZ-based cell showed a stable voltage output that decreased only slightly over 300 h. However, the voltage of the SCF-based cell decreased to zero after 24 h. This result indicates that Zr-doping greatly improved the stability of the cell.

The insets in Fig. 11 show the cross-sectional microstructure of the pristine and post-test cells. The thicknesses of the densified BZCYyb electrolyte layer and SCFZ cathode layer were approximately 38 μm and 30 μm , respectively. Compared to the pristine cell, the cathode particles of the post-test cell showed obvious aggregation. Simultaneously, the cathode layer was well-adhered to the electrolyte layer, indicating good thermal compatibility between SCFZ and BZCYyb.

Conclusions

Perovskite-type oxide SCFZ was prepared via a modified Penichi method and investigated as a CO_2 tolerant cathode based on the electrolyte BZCYyb for IT-SOFCs. Doping 5 mol% Zr into SCF formed a stabilized cubic perovskite structure. In addition, SCFZ showed good chemical compatibility with the electrolyte BZCYyb under the working conditions of SOFCs and good electrical conductivities of $202\text{--}345 \text{ S cm}^{-1}$ from 700 to 400 °C . The cell with the SCFZ cathode demonstrated a peak output of 712 mW cm^{-2} at 700 °C and a long-term stability over at least 300 h, which indicated that SCFZ is a potential cathode candidate for IT-SOFCs with the electrolyte BZCYyb.

Conflicts of interest

There are no conflicts to declare.

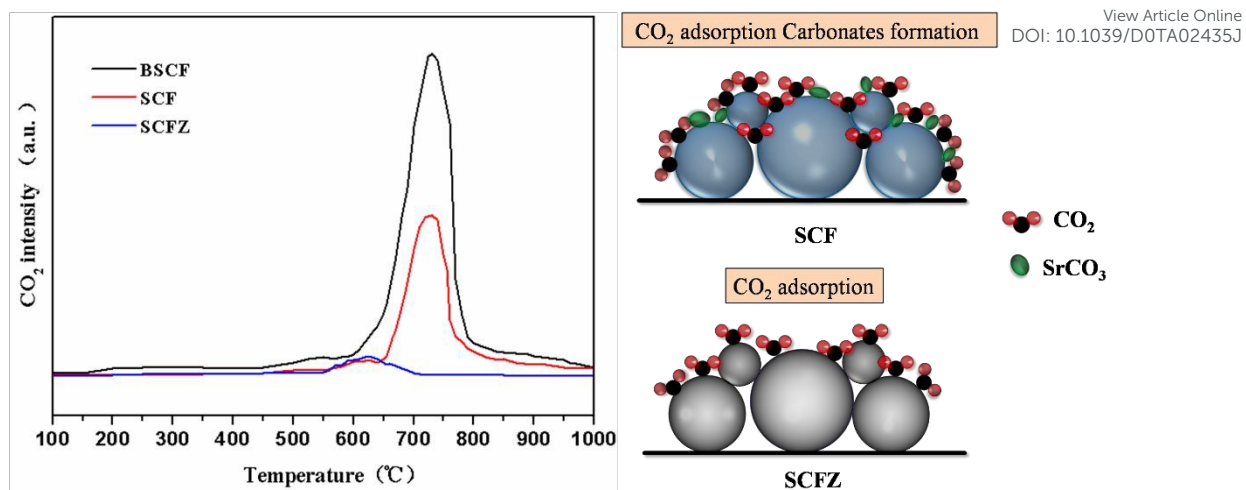
Acknowledgements

This work was supported by the Central Government's Special Fund for Local Science and Technology Development (YDZX20191400002916); Coal Seam Gas Joint Foundation of Shanxi (2015012016); Shanxi "1331 Project" Engineering Research Center (PT201807) and Key Innovative Research Team; Shanxi Province Science Foundation (2016011025); Shanxi Scholarship Council of China (2016-010); The innovation team construction plan of "1331 project" of Jinzhong University (jzycxtd2019010).

Notes and references

- 1 B. C. H. Steele and A. Heinzel, *Nature*, 2001, **414**, 345-352.
- 2 N. Mahato, A. Banerjee, A. Gupta, S. Omar, and K. Balani, *Prog. Mater. Sci.*, 2015, **72**, 141-337.
- 3 D. J. L. Brett, A. Atkinson, N. P. Brandon and S. J. Skinner, *Chem. Soc. Rev.*, 2008, **37**, 1568-1578.
- 4 E. D. Wachsman and K. T. Lee, *Science*, 2011, **334**, 935-939.
- 5 Z. Gao, L. V. Mogni, E. C. Miller, J. G. Railsback and S. A. Barnett, *Energy Environ. Sci.*, 2016, **9**, 1602-1644.

- 6 B. Singh, S. Ghosh, S. Aic and B. Roy, *J. Power Sources*, 2017, **339**, 103-135.
- 7 S. Hossain, A. M. Abdalla, S. N. B. Jamain, J. H. Zaini and A. K. Azad, *Renewable and Sustainable Energy Reviews*, 2017, **79**, 750-764.
- 8 E. Fabbri, D. Pergolesi and E. Traversa, *Chem. Soc. Rev.*, 2010, **39**, 4355-4369.
- 9 L. Yang, S. Z. Wang, K. Blinn, M. F. Liu, Z. Liu, Z. Cheng and M. L. Liu, *Science*, 2009, **326**, 126-129.
- 10 Y. Liu, L. Yang, M. F. Liu, Z. Y. Tang and M. L. Liu, *J. Power Sources*, 2011, **196**, 9980-9984.
- 11 B. B. He, L. Zhang, Y. X. Zhang, D. Ding, J. M. Xu, Y. H. Ling and L. Zhao, *J. Power Sources*, 2015, **287**, 170-176.
- 12 S. B. Adler, *Chem. Rev.*, 2004, **104**, 4791-4843.
- 13 Z. P. Shao, W. Zhou and Z. H. Zhu, *Prog. Mater. Sci.*, 2012, **57**, 804-874.
- 14 Y. B. Chen, W. Zhou, D. Ding, M. L. Liu, F. Ciucci, M. Tade and Z. P. Shao, *Adv. Energy Mater.*, 2015, **5**, 1500537.
- 15 D. J. Chen, C. Chen, Z. B. Zhang, Z. M. Baiyee, F. Ciucc and Z. P. Shao, *ACS Appl. Mater. Interfaces*, 2015, **7**, 8562-8571.
- 16 J. Sunarso, S. Baumann, J. M. Serra, W. A. Meulenber, S. Liu, Y. S. Lin and J. C. Diniz da Costa, *J. Membr. Sci.*, 2008, **320**, 13-41.
- 17 M. R. Li, W. Zhou and Z. H. Zhu, *Asia-Pac. J. Chem. Eng.*, 2016, **11**, 370-381.
- 18 W. H. Wang, Y. Yang, D. M. Huan, L. K. Wang, N. Shi, Y. Xie, C. R. Xia, R. R. Peng and Y. L. Lu, *J. Mater. Chem. A*, 2019, **7**, 12538-12546.
- 19 C. A. Hancock, R. C. T. Slade, J. R. Varcoe and P. R. Slater, *J. Solid State Chem.*, 2011, **184**, 2972-2977.
- 20 H. Kruidhof, H. J. M. Bouwmeester, R. H. E. v. Doorn and A. J. Burggraaf, *Solid State Ionics*, 1993, **63-65**, 816-822.
- 21 Z. P. Shao and S. M. Haile, *Nature*, 2004, **431**, 170-173.
- 22 T. Nagai, W. Ito and T. Sakon, *Solid State Ionics*, 2007, **177**, 3433-3444.
- 23 S. F. Wang, Y. F. Hsu, C. T. Yeh, C. C. Huan and H. C. Lu, *Solid State Ionics*, 2012, **227**, 10-16.
- 24 P. Y. Zeng, R. Ran, Z. H. Chen, W. Zhou, H. X. Gu and Z. P. Shao, *J. Alloys and Compounds*, 2008, **455**, 465-470.
- 25 H. Y. Liu, X. F. Zhu, Y. Cong, T. Y. Zhang and W. S. Yang, *Phys. Chem. Chem. Phys.*, 2012, **14**, 7234-7239.
- 26 N. Grunbaum, L. Moggi, F. Prado and A. Caneiro, *J. Solid State Chem.*, 2004, **177**, 2350-2357.
- 27 L. M. Liu, T. H. Lee, L. Qiu, Y. L. Yang and A. J. Jacobson, *Mater. Res. Bull.*, 1996, **31**, 29-35.
- 28 Z. F. Wang, H. L. Zhao, N. S. Xu, Y. N. Shen, W. Z. Ding, X. G. Lu and F. S. Li, *J. Physics and Chemistry of Solids*, 2011, **72**, 50-55.
- 29 T. Klande, O. Ravkina and A. Feldhoff, *J. Membr. Sci.*, 2013, **437**, 122-130.
- 30 L. Shao, F. Z. Si, X. Z. Fu and J. L. Luo, *Int. J. Hydrogen Energy*, 2018, **43**, 7511-7514.
- 31 W. Chen, C. S. Chen and L. Winnubst, *Solid State Ionics*, 2011, **196**, 30-33.
- 32 X. F. Ding, Z. P. Gao, D. Ding, X. Y. Zhao, H. Y. Hou, S. H. Zhang and G. L. Yuan, *Appl. Catal. B: Environ.*, 2019, **243**, 546-555.
- 33 V. Cascos, M. T. Fernandez-Díaz and J. A. Alonso, *Renewable Energy*, 2019, **133**, 205-215.
- 34 B. P. Qu, W. Long, F. J. Jin, S. Z. Wang and T. M. He, *Int. J. Hydrogen Energy*, 2014, **39**, 12074-12082.
- 35 V. Cascos, L. Troncos and J. A. Alonso, *Int. J. Hydrogen Energy*, 2015, **40**, 11333-11341.
- 36 A. J. Fernández-Ropero, J. M. Porras-Vázquez, A. Cabeza, P. R. Slater, D. Marrero-López and E. R. Losilla, *J. Power Sources*, 2014, **249**, 405-413.
- 37 L. Yang, L. Tan, X. H. Gu, W. Q. Jin, L. X. Zhang and N. P. Xu, *Ind. Eng. Chem. Res.*, 2003, **42**, 2299-2305.
- 38 X. X. Meng, N. T. Yang, B. Meng, X. Y. Tan, Z. F. Ma and S. M. Liu, *Ceram. Int.*, 2011, **37**, 2701-2709. DOI: 10.1039/D0TA02435J
- 39 H. Lu, Z. Q. Deng, J. H. Tong and W. S. Yang, *Materials Letters*, 2005, **59**, 2285-2288.
- 40 L. dos Santos-Gómez, J. M. Compana, S. Bruque, E. R. Losill and D. Marrero-López, *J. Power Sources*, 2015, **279**, 419-427.
- 41 M. Shang, J. H. Tong and R. O'Hayre, *RSC Adv.*, 2013, **3**, 15769-15775.
- 42 C. C. Duan, D. Hook, Y. C. Chen, J. H. Tong and R. O'Hayre, *Energy Environ. Sci.*, 2017, **10**, 176-182.
- 43 R. Zohourian, R. Merkle and J. Maier, *Solid State Ionics*, 2017, **299**, 64-69.
- 44 A. Afif, N. Radenahmad, C. M. Lim, M. I. Petra, M. A. Islam, S. M. H. Rahman, S. Eriksson and A. K. Azad, *Int. J. Hydrogen Energy*, 2016, **41**, 11823-11831.
- 45 S. Z. Wang, F. J. Jin, L. Li, R. R. Li, B. P. Qu and T. M. He, *Int. J. Hydrogen Energy*, 2017, **42**, 4465-4477.
- 46 Z. F. Wang, H. L. Zhao, N. S. Xu, Y. N. Shen, W. Z. Ding, X. G. Lu and F. S. Li, *J. Physics and Chemistry of Solids*, 2011, **72**, 50-55.
- 47 S. Carter, A. Selcuk, R. J. Chater, J. Kajda, J. A. Kilner and B. C. H. Steele, *Solid State Ionics*, 1992, **53-56**, 597-605.
- 48 H. Hayash, M. Watanabe, M. Ohuchida, H. Inaba, Y. Hiei, T. Yamamoto and M. Mori, *Solid State Ionics*, 2001, **144**, 301-313.
- 49 C. de. la. Calle, A. Aguadero, J. A. Alonso and M. T. Fernández-Díaz, *Solid State Sci.*, 2008, **10**, 1924-1935.
- 50 L. M. Zhang, J. Shan and Q. Wang, *J. Alloys and Compounds*, 2019, **771**, 221-227.
- 51 L. W. Tai, M. M. Nasrallah, H.U. Anderson, D.M. Sparli and S.R. Sehlin, *Solid State Ionics*, 1995, **76**, 273-283.
- 52 H. Patra, S.K. Rout, S.K. Pratihar and S. Bhattacharya, *Int. J. Hydrogen Energy*, 2011, **36**, 11904-11913.
- 53 B. B. Gu, J. Sunarso, Y. Zhang, Y. F. Song, G. M. Yang, W. Zhou and Z. P. Shao, *J. Power Sources*, 2018, **405**, 124-131.
- 54 A. Y. Yan, M. Yang, Z. F. Hou, Y. L. Dong and M. J. Cheng, *J. Power Sources*, 2008, **185**, 76-84.
- 55 M. R. Li, W. Zhou and Z. H. Zhu, *ACS Appl. Mater. Interfaces*, 2017, **9**, 2326-2333.



5 mol% zirconium was introduced into SrCo_{0.8}Fe_{0.2}O_{3-δ} (SCF) to promote its structural stability and CO₂ tolerance. The proton-conducting solid oxide fuel cells (H⁺-SOFCs) with SCFZ material as a cathode showed a high output and durability.